



HAL
open science

Quantitative risk assessment in El-Jadida (Northern Atlantic Coast of Morocco) for a tsunami scenario equivalent to that of the 1755 Lisbon earthquake

Abdelkarim Tadibaght, Kamal Agharroud, Ali Bounab, Abdelmounim El M'rini, Lionel Siame, Younes El Kharim, Olivier Bellier, Otman El Ouaty

► To cite this version:

Abdelkarim Tadibaght, Kamal Agharroud, Ali Bounab, Abdelmounim El M'rini, Lionel Siame, et al.. Quantitative risk assessment in El-Jadida (Northern Atlantic Coast of Morocco) for a tsunami scenario equivalent to that of the 1755 Lisbon earthquake. *Environmental Earth Sciences*, 2022, 81 (5), pp.163. 10.1007/s12665-022-10277-0 . hal-03662616

HAL Id: hal-03662616

<https://hal.science/hal-03662616>

Submitted on 16 Jun 2022

HAL is a multi-disciplinary open access archive for the deposit and dissemination of scientific research documents, whether they are published or not. The documents may come from teaching and research institutions in France or abroad, or from public or private research centers.

L'archive ouverte pluridisciplinaire **HAL**, est destinée au dépôt et à la diffusion de documents scientifiques de niveau recherche, publiés ou non, émanant des établissements d'enseignement et de recherche français ou étrangers, des laboratoires publics ou privés.

1 **Quantitative risk assessment in El-Jadida (Northern Atlantic Coast of**
2 **Morocco) for a tsunami scenario equivalent to that of the 1755 Lisbon**
3 **earthquake**

4 Abdelkarim Tadibaght^{1*}, Kamal Agharroud², Ali Bounab², Abdelmounim El M'rini¹, Lionel Siame³, Younes El
5 Kharim², Olivier Bellier^{3,4}, Otman El Ouaty¹

6 ¹ LR3G, FS, Abdelmalek Essaadi University, Tétouan, Morocco

7 ² GERN, FS, Abdelmalek Essaadi University, Tétouan, Morocco

8 ³ Aix Marseille Univ, CNRS, IRD, INRAE, Coll France, CEREGE, Aix-en-Provence, France

9 ⁴ Aix Marseille Univ, CNRS, ECCOREV, Aix-en-Provence, France

10 * Address correspondence to Abdelkarim Tadibaght

11 E-mail: tadibaghtabde@gmail.com/Tel: +212657966260/Orcid: <https://orcid.org/0000-0001-7161-0154>

12 Kamal Agharroud Orcid: <https://orcid.org/0000-0002-2079-4245>

13 Ali Bounab Orcid: <https://orcid.org/0000-0002-3411-3930>

14 Abdelmounim El M'rini Orcid: <https://orcid.org/0000-0002-7963-5660>

15 Lionel Siame Orcid: <https://orcid.org/0000-0002-4288-9528>

16 Younes El Kharim Orcid: <https://orcid.org/0000-0001-9451-3955>

17 Olivier Bellier Orcid: <https://orcid.org/0000-0002-3213-7306>

18 Otman El Ouaty Orcid: <https://orcid.org/0000-0003-0593-4358>

19 **Abstract**

20 The Atlantic coasts of Morocco are exposed to tsunami risk. Although this risk level is low because of
21 the rarity of tsunamis in the region, a future event would be catastrophic for the Moroccan society and economy
22 because of the numerous issues at stake. In this paper, bathymetric/topographic data and parameters of three
23 known tsunamigenic faults (Marquês do Pombal Fault, Gorringe Bank Fault and Horseshoe Fault) were used to
24 simulate a potential tsunami event in the city of El-Jadida (Morocco) using MIRONE software. The simulation
25 results of the worst-case scenario were then exploited to perform a quantitative risk assessment, using
26 demographic and economic input data. Results show that choosing the Horseshoe Fault as source of the
27 simulated event produces the largest tsunamis; with maximum wave heights ranging from 10 m to 27 m. These
28 results are found to be consistent with historical records and computer model simulations from previous studies.
29 Quantitative risk assessment results indicate that the city of El-Jadida is exposed to a high risk of loss of lives
30 and properties with values of the order of 34 lives/yr and 14M\$/yr respectively. For this reason, we underline the
31 dire need for the implementation of tsunami risk prevention and mitigation strategies that should prioritize the
32 protection of high-risk areas of the city and its population from a possible future catastrophic event.

33 **Keywords:** Tsunami, Simulation, Quantitative Risk Assessment, Atlantic coasts, Morocco.

34 **1. Introduction**

35 Tsunami is one of the deadliest natural hazards, claiming hundreds of thousands of lives all around the
36 world (e.g., Bernard *et al.* 1988; Doocy *et al.* 2007). In addition, tsunami events also constitute a great risk to
37 coastal regions increasingly impacted by different human activities. For instance, the tsunami of December 26th
38 2004 killed more than 300 000 people and caused economic damage exceeding \$10 billion to countries
39 surrounding the Indian Ocean (Sharpley 2005). This disaster has spurred scientific research with aim of better
40 understanding tsunamis and their potential economic, environmental and societal impacts.

41 In the Gulf of Cadiz (Fig.1), with the exception of some small tsunami waves generated by the 1969 earthquake
42 (Baptista *et al.* 1992), no tsunami events were experienced during course of the twentieth century. However, the
43 massive destruction caused by tsunami waves associated with the historical 1755 Lisbon earthquake (Levret
44 1991), strongly highlights the exposure of the this region to this hazard and its proneness to produce catastrophic
45 events in the future (Baptista *et al.* 1998; Gutscher *et al.* 2006).

46 To simulate possible future occurrences, computer models were run based on the characteristics of potential
47 tsunamigenic seismic sources located in the Gulf of Cadiz (e.g. Barkan *et al.* 2009; Font *et al.* 2010). In all of
48 these studies, the destructiveness of probable future tsunamis for the U.S, Spanish and Portuguese coasts was
49 demonstrated. From a socioeconomic point of view, such events would be disastrous for Morocco as well, given
50 that a large portion of its population (10.3 million people) (Laouina 2019), and large segments of its economy
51 are tied to important coastal cities alongside its Atlantic shoreline. For this reason, several studies have attempted
52 to evaluate the impact of a potential tsunami on some of the populous (i.e., Casablanca, Rabat and El-Jadida; see
53 for example Omira *et al.* 2009; Mellas *et al.* 2012; Moussaoui *et al.* 2017), but these studies have been limited to
54 qualitative risk assessments. Such methods are subjective and lack a numerical basis for the estimation of
55 potential economic and societal losses. Conversely, Quantitative Risk Assessment (QRA) methods are more
56 objective and produce more realistic estimations of the tsunami impact because they elicit measurable
57 quantitative data from experts, without simply relying on the expert's opinion (Jelínek and Krausmann 2008).

58 To choose one approach over the other, one has to consider the objectives of the study. In fact, qualitative risk
59 assessment methods are limited to national and regional scale zonation efforts aiming to determine high risk
60 areas on which quantitative assessments need to be performed using higher resolution data. The latter approach
61 is found to be more useful for decision makers since it allows a better risk-to-reward assessment for planning and
62 funding of mitigation strategies and programs (Saunders and Glassey 2007). In scenario based QRA studies
63 conducted from a human perspective, one has to first characterize the spatio-temporal hazard, then estimate the
64 issues at stake and finally assess their vulnerability to the catastrophic event (Granger *et al.* 1998; Papathoma *et al.*
65 *et al.* 2003; Nadim 2006; Post *et al.* 2009; Jelínek *et al.* 2012). For tsunami hazard characterization, the mapping of
66 tsunamogenic faults (source area) and tsunami propagation geometry can be performed using a variety of
67 simulation softwares, while the vulnerability assessment can be done using different methods, depending on the
68 objectives of the study and data availability.

69 In effect, to conduct an accurate QRA, simulation results obtained using a robust algorithm must be used as input
70 data. However, most tsunami simulation softwares are expensive and thus not accessible to all researchers,
71 especially in developing countries. Conversely, MIRONE simulation software, which is a free and open-source
72 alternative capable of simulating tsunami events with reasonable accuracy (Luis 2007), constitutes a cost-
73 effective alternative to model tsunami wave propagation and wave heights both offshore and on land. This tool
74 adopts the Mansinha and Smylie (1971) equation which uses fault geometry, the bathymetry of the area and the

75 triggering earthquake magnitude as input data. Such information can be drawn from previous geological studies
76 as well as digital elevation models available online.

77 QRA only measures the immediate damage caused by a given tsunami, without taking into consideration post-
78 disaster rescue operations, and their role in aggravating or diminishing the overall death toll and number of
79 missing people. This was demonstrated in the 2004 tsunami where patient transport efforts and medical rescue
80 coordination and infrastructure allowed rescuing hundreds of lives (Li and Zheng 2014).

81 In this paper, we conducted a tsunami simulation using MIRONE, combined with demographic and economic
82 data to establish a QRA for the city of El-Jadida (Fig.1). This area was chosen because it was devastated by
83 tsunami waves generated during the 1755 Lisbon event, as reported by Soyris (1755). The aim of this paper is to
84 propose a time-saving low-cost tsunami QRA method capable of helping decision makers to develop better
85 strategies for tsunami risk mitigation, based on objective and quantifiable datasets.

86 **2. Study area :**

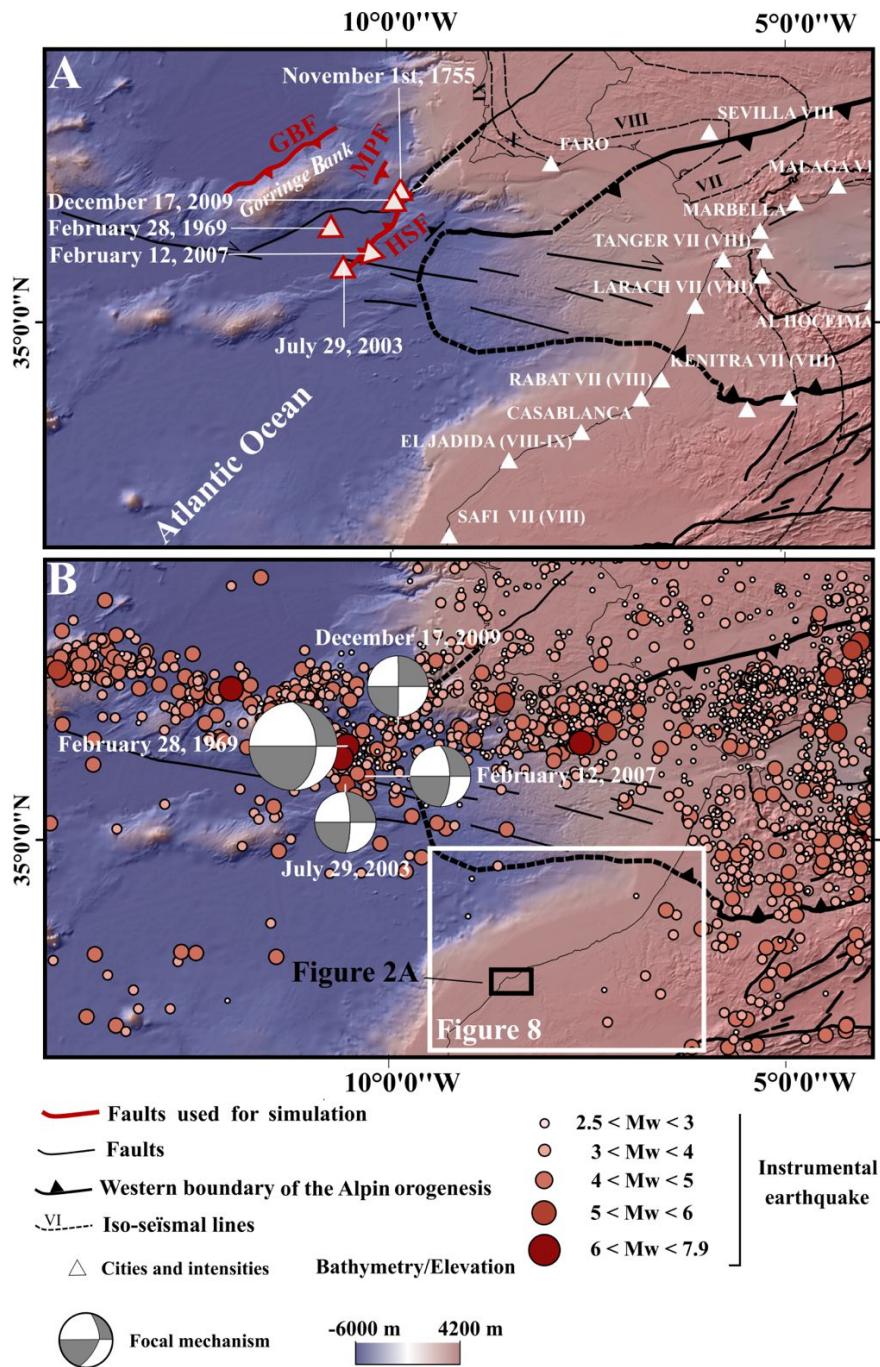
87 **2.1. Seismic setting and tsunamigenic faults in the Gulf of Cadiz.**

88 The Gulf of Cadiz is characterized by a high-level of seismic activity related to convergence at the
89 poorly defined, Eurasia-Africa plate boundary (Fig. 1A) (e.g. Matias *et al.* 2013). In some cases, regional seismic
90 events can generate large tsunamis, such as the Lisbon earthquake of 1755 ($M = 8.5-9$), which is considered the
91 strongest ever recorded seismic event in western Europe (Fig. 1B) (Levret 1991; Baptista *et al.* 1998; Gutscher *et*
92 *al.* 2006). Despite a significant magnitude ($M_w = 7.8$) (Fukao 1973), the second largest seismic event that struck
93 the Gulf of Cadiz and its surrounding coasts in 1969 only generated small tsunamis waves (Baptista *et al.* 1992).
94 More recently, some lower-magnitude seismic events occurred in 2003 ($M_w = 5.3$), 2007 ($M_w = 5.9$) and 2009
95 ($M_w = 5.5$), but they did not generate tsunamis in the region (Pro *et al.* 2013). Following these events, no
96 earthquake with M_w greater than 6 has been recorded (Matias *et al.* 2013).

97 In the Gulf of Cadiz, instrumental earthquake data show that the region is tectonically active with most focal
98 points being concentrated alongside active faults in the region (Fig. 1). The focal mechanisms retrieved from the
99 Harvard Global centroid moment tensor catalogue (Ekström *et al.* 2012), show that most events, which can be
100 related to the same tectonics responsible for the 1755 event, are caused by compound reverse strike-slip or pure
101 strike-slip motion (Fig.1) (e.g. Pro *et al.* 2013).

102 The locations of some of the recent earthquake epicenters can be determined with more accuracy (Fig. 1).
103 Nevertheless, that of the 1755 event is still a matter of debate in the scientific community. To tackle this,

104 intensity maps of the 1755 earthquake were compared to those of the 1969 event (e.g. Levret 1991; Buform et al.
105 2020) and to macro-seismic (Solares and Arroyo 2004) and micro-seismic (Silva et al., 2017) data recorded
106 during the twentieth century. The findings of these studies suggest that the most probable epicenter location of
107 the 1755 event is to the southwest of Cape Saint-Vincent (Fig.1), and that the 1969 and 1755 could be associated
108 with the same seismogenic source (Levret 1991). However, according to Johnston (1996) and Hayward et al.
109 (1999) the 1755 epicenter location could also be the Gorringe Bank because of the presence of active NNE to NE
110 trending thrust faults related to submarine tectonic uplift (Gorringe Bank Fault). The region of Marquês do
111 Pombal also qualifies as a possible location for the Lisbon event's epicenter, where an active fault could be a
112 potential source (Zitellini et al. 1999, 2001). In addition, the seismicity is also not spatially correlated with
113 surficial fault zones in this area, (deep earthquakes 20 to 40 km). Yet, Buform et al. (2020) suggested that the NE
114 trending thrust fault known as the Horseshoe Fault, which is characterized by a continual occurrence of seismic
115 events (2003, 2007 and 2009) (Pro et al. 2013) (Fig.1), is much more likely to be the source of the 1755
116 tsunamigenic earthquake.



117

118 Figure 1: Geodynamic setting of the Gulf of Cadiz and its surrounding areas. (A) Major active structures
 119 proposed as the possible source of the 1755 tsunamigenic earthquake event (GBF, Goringe Bank Fault; MPF,
 120 Marquês do Pombal Fault; HSF, Horseshoe Fault), associated with isoseismic lines (MSK Scale) showing its
 121 effects on the Moroccan and Iberian regions (from Levret 1991). Red triangles indicate the location of
 122 earthquake events discussed in this section. (B) Seismotectonic map of the Gulf of Cadiz and its surrounding
 123 areas. The instrumental data is from International Seismological Center (2020) and focal mechanisms from
 124 Harvard global centroid moment tensor catalog (Ekström et al. 2012). Locations of figures 2 and 8 are shown.

125 **2.2. Tsunamis in Morocco**

126 Morocco is vulnerable to coastal hazards because its most economically influential cities are located
127 alongside its Atlantic and Mediterranean shorelines. In addition to storms, coastal erosion, and sea level rise,
128 tsunamis constitute the most dangerous coastal hazard threatening these newly-constructed human settlements in
129 the area (Blanc 2009; Omira *et al.* 2010; Atillah *et al.* 2011; Renou *et al.* 2011). In fact, the impact of past
130 occurrences, such as that of 1755, have been documented in old towns that have now grown into big cities close
131 to, or on, the Atlantic shoreline (El Mrabet 2005; Blanc 2009). Several attempts to model the effects of these
132 events and to estimate the risk to human life and goods, show that the region is widely exposed if similar events
133 were to recur (Omira *et al.* 2010; Atillah *et al.* 2011; Renou *et al.* 2011; Mellas *et al.* 2012; Moussaoui *et al.*
134 2017; Ramalho *et al.* 2018). In addition to historical documents, material evidence (geomorphic and sedimentary
135 indices) for tsunamis or high energy events in Morocco have been found in many sites alongside the Moroccan
136 Atlantic coast: (1) in Larache and Rabat (Medina *et al.* 2011), (2) Tahadart estuary (Talibi *et al.* 2016; Khalfaoui
137 *et al.* 2020) and (3) close to the Loukkos river mouth, (Mhammdi and Medina, 2015). According to Soyris
138 (1755), the Lisbon earthquake of 1755, the intensity of which reached VIII-XI on the Mercali scale, produced a
139 large tsunami wave that affected northern Morocco, with El-Jadida city being one of the most impacted (Levret
140 1991). Other descriptive data, as well as tsunami hazard assessments performed using simulations agree on the
141 great impact of this event on El-Jadida city (e.g. Blanc 2009; Ramalho *et al.* 2018).

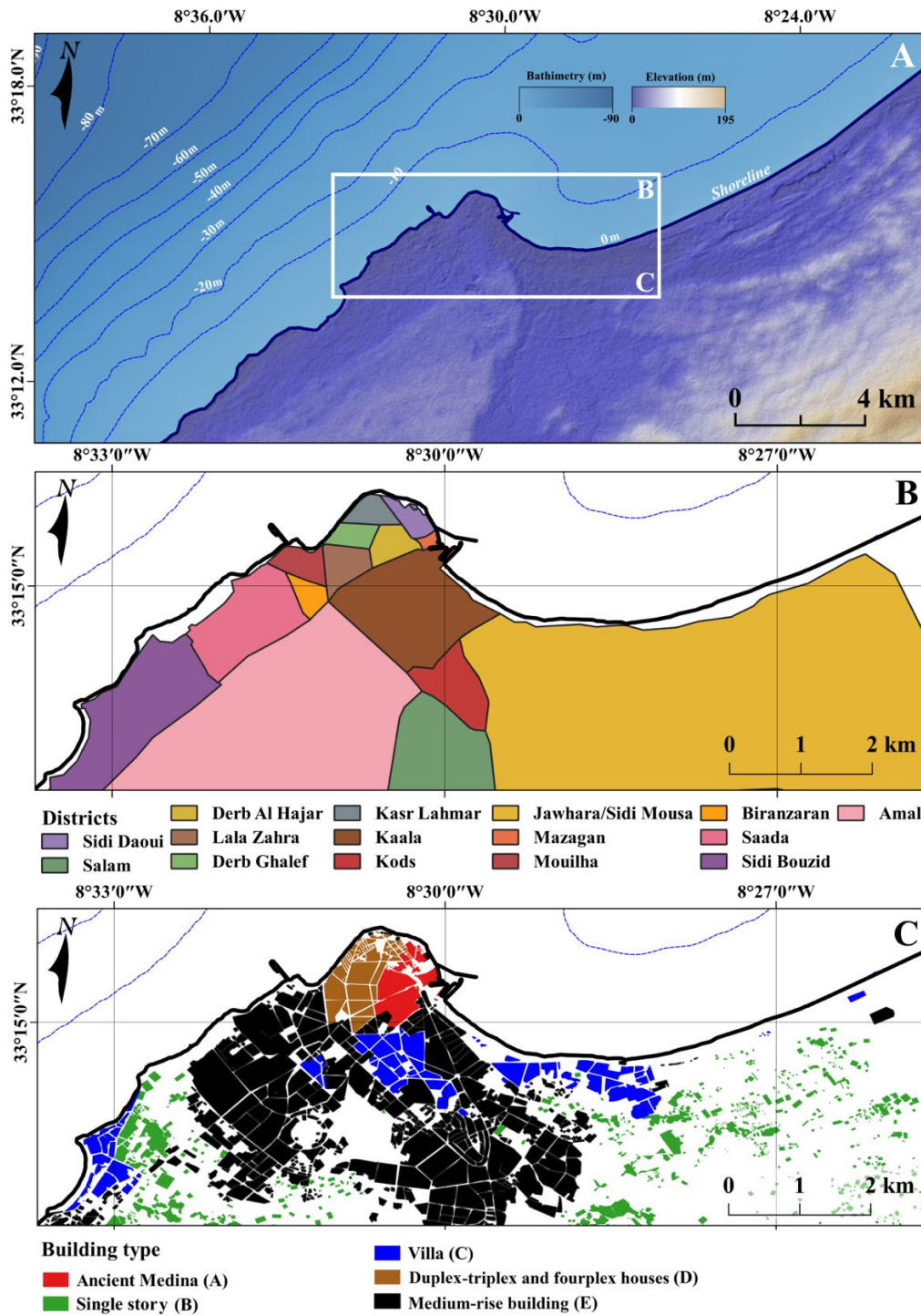
142 **2.3. Socio-economic setting of El-Jadida**

143 The largest and most important cities for the Moroccan economy (nearly 66% of its total Gross
144 Domestic Product (GDP)) are located along its Atlantic coast (D.A.T. 2017). As such, any tsunami should have a
145 long-lasting catastrophic impact on the economy of the country. Nevertheless, despite natural disasters causing
146 negative economic consequences in most areas of the world, and at best a full recovery and return to the previous
147 state of affairs after years to few decades (Cavallo *et al.* 2013), some events can trigger economic growth by
148 generating aid from international institutions and governments. A fine example is the Asian tsunami of 2004,
149 which turned out to be an iconic case of international cooperation and solidarity in the face of natural
150 catastrophes (Cavallo and Noy 2011; Loayza *et al.* 2012; Heger and Neumayer 2019).

151 El-Jadida city is characterized by a high level of exposure and vulnerability to tsunami events because of : (1)
152 the poor design of its marine defense structures (Omira *et al.* 2013); (2) its high population density with ≈ 7000
153 inhabitants/km² (H.C.P. 2014); (3) the low level of education (86.5 % of El-Jadida population is below level 3 of

154 the international education standard, 23.3 % being illiterate (H.C.P. 2014); (4) the relatively high percentage of
155 residents aged 55 or older (13% of El-Jadida's, i.e. for 25,000 people (H.C.P. 2014); (5) and the fact that most of
156 El-Jadida's buildings are located within 3 km from the Atlantic shoreline, on relatively flat terrain (Fig. 2).

157 Regarding construction practices in the study area, all buildings can be grouped into five major categories based
158 on practices and materials, the number of storeys and the reference unit-price for each square meter (Fig. 2-C,
159 Fig.3 and Fig.4). The first type (ancient Medina), which dominates in Cape Mazagan, dates back to the Middle
160 Ages and differs considerably from other districts (UNESCO 2004). Despite its oldness, the Mazagan district can
161 be considered as one of the least vulnerable sites because it was built on relatively elevated land (altitude > 6 m)
162 (Fig.4-f). Other newly built districts are constructed using reinforced concrete and do not have any protection
163 against coastal hazards (Fig. 3).



164

165 Figure 2: (A) Topography of El-Jadida city and surrounding areas and offshore bathymetry. Topography from
 166 the ALOS PALSAR Digital elevation model is used (<https://search.asf.alaska.edu>, accessed December 2020),
 167 and bathymetry extracted from the GEBCO database
 168 (https://www.gebco.net/data_and_products/gridded_bathymetry_data/, accessed December 2019) (B) Spatial
 169 distribution of El-Jadida city districts. (C) Spatial distribution of El-Jadida building types
 170 (<https://maps.google.com>, accessed December 2020).



171

172 Figure 3: The beach topography of El-Jadida city and the location of major building types, which represent the
 173 first elements to face the tsunami hazard.

174 In addition, the construction types greatly influence the population density values. For instance, villas (Fig.4-c)
 175 are characterized by a very low population density, in contrast to the ancient medina (Fig.4-a) and medium-rise-
 176 buildings (Fig.4-e). As for single storeys, duplex-triplex and fourplex houses (Fig.4-b-d), a lower density is also
 177 expected.

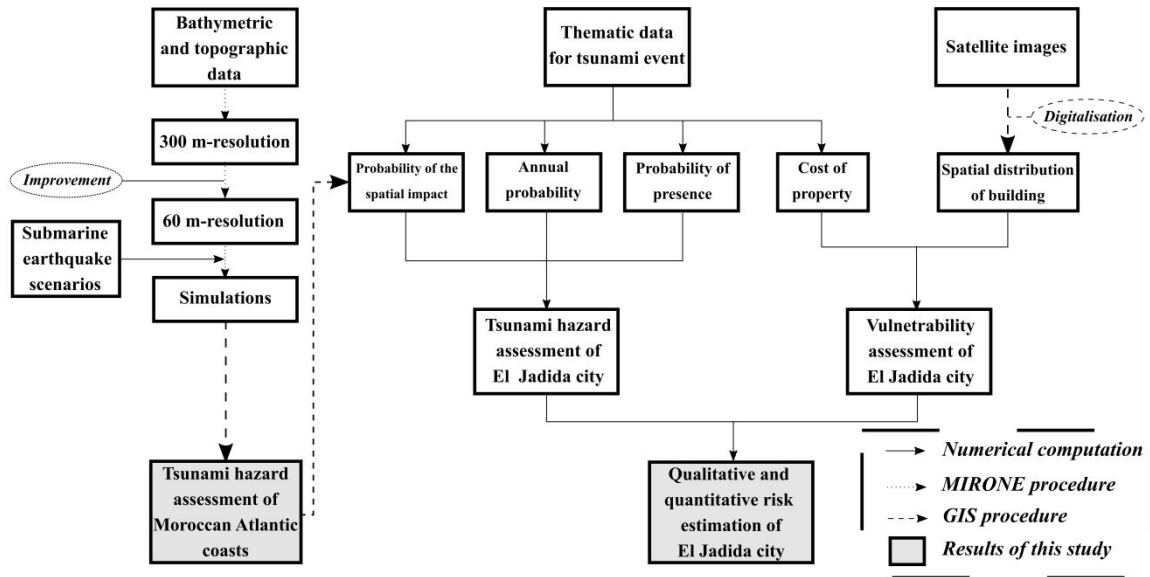


178

179 Figure 4: The main types of building types of El-Jadida city: (a) ancient Medina; (b) single-story buildings; (c)
 180 villa; (d) duplex-triplex and fourplex houses; (e) medium-rise buildings; (f) the marine protection wall of the
 181 ancient Medina.

182 **3. Material and Methods**

183 In this study, we adopted a new approach to QRA (Fig. 5), based on the exploitation of simulation results to
 184 assess tsunami risk calculate using the Fell et al. (2005) assessment system.



185
 186 Figure 5: Logical approach adopted to evaluate the tsunami risk in El-Jadida city, seismic scenarios and tsunami
 187 generations.

188 **3.1. Tsunami simulation**

189 To evaluate the impact of a future tsunami event on El-Jadida city, three tsunamigenic faults were
 190 considered as potential sources (Table.1) (Blanc 2009). The Gorringe Bank Fault, the Marquês do Pombal Fault,
 191 and the Horseshoe Fault (see section 2.1). These faults are submarine structures located offshore in the Gulf of
 192 Cadiz, a region known for its seismotectonic activity (Hayward et al. 1999; Zitellini et al. 2001; Gràcia et al.
 193 2003; Cunha et al. 2010), its seismo-stratigraphic signature (e.g. Bartolome et al. 2012; Martínez-Loriente et al.
 194 2018), and an abundance of instrumental seismic data (ISC2020).

195 To model potential tsunamis waves generated by these faults, we used MIRON simulation software (Luis
 196 2007), which employs the Mansinha equation (Mansinha and Smylie 1971) to generate these waves (using the
 197 elastic deformation tools), and the TINTOL code to simulate their propagation in the Gulf of Cadiz as well as
 198 their inundation impact along the El-Jadida coastline. A rectangle, based on fault lengths and length/width ratios,
 199 was used to simplify the geometry of the faults and to fix the slip amplitude accordingly (Scholz 1981). Using

200 the faults parameters, the magnitude for each earthquake scenario (Table. 1) is automatically computed by the
201 numerical simulation software. The equation is the seismic moment's formula (Eq.1 and Eq.2) (Aki 1966):

$$202 \quad M_0 = \mu \times A \times D \quad (1)$$

203 Where D is coseismic displacement, A is the rupture area (km²) and μ is the crustal rigidity coefficient (Nm⁻²).
204 To the magnitude of the event, MIRONE adopts the M_0 - M_w equation (Hanks and Kanamori 1979):

$$205 \quad \text{Log}_{10} (M_0) = 1.5 \times M_w + 9.05 \quad (2)$$

206 Where M_0 is the seismic moment (Nm) and M_w the moment magnitude.

207 The bathymetric/topographic data used for this simulation were downloaded from the GEBCO database (General
208 Bathymetric Chart of the Oceans, https://www.gebco.net/data_and_products/gridded_bathymetry_data/ ,
209 accessed December 2019). The computation was performed using 0.8s time steps for a total duration of 6120s.
210 This dataset is nested for consecutive calculations of tsunami generation and propagation in an open boundary
211 condition as well as inland inundation.

212 The MIRONE software uses a nested grid system with different grid resolutions in order to generate tsunami
213 simulations at various spatial resolutions. The main grid has a 300m-resolution and was used for tsunami
214 propagation in the Gulf of Cadiz. The second grid, improved by transplanting the main grid using 'transplant 2nd
215 grid tool'(Luis 2007), has a 60m-resolution and was used for inland inundation at El-Jadida. The outputs of the
216 simulations are raster maps of the flooded areas featuring the maximum wave height for each pixel (see section
217 4.1).

218

219

220

221

222

223 Table 1: Active fault parameters used to simulate tsunamigenic scenarios in the Gulf of Cadiz (modified from
 224 Omira et al. 2009). L: the length of the fault; W: the width of the fault; μ : the crustal rigidity and M_w : the
 225 moment magnitude.

	Dimension (km)		Fault parameters						
	L	W	Depth (km)	Slip (m)	Strike ($^{\circ}$)	Dip ($^{\circ}$)	Rake ($^{\circ}$)	μ ($\times 10^{10}$ Nm $^{-2}$)	M_w
Source									
Gorringe Bank Fault	127	60	5	8.3	233	35	90	3.0	8.2
Marquês do Pombal Fault	129	70	4	8	20	35	90	3.0	8.2
Horseshoe Fault	165	70	4	10.7	42.1	35	90	3.0	8.4

226

227 **3.2. Quantitative Risk Assessment (QRA)**

228 Although three scenarios were used for the simulation, only the one with the Horseshoe Fault defined as the
 229 source was retained for QRA (Table.1). This scenario was chosen because this fault has been responsible for
 230 many events of significance in recent years (Pro et al. 2013), and it was linked in many studies to the 1755
 231 tsunamigenic earthquake (Fig.1-A) (e.g. Solares and Arroyo 2004). In addition, this scenario is also expected to
 232 produce the biggest waves (e.g. Omira et al. 2009).

233 To perform the QRA calculations, the equations system from Fell et al. (2005) was used since it takes into
 234 consideration both the natural hazard aspects and the socio-economic characteristics of a given area. This set of
 235 equations allows calculating two types of risk: the annual risk of loss of property and the annual risk of loss of
 236 life.

237 **3.2.1. Annual risk of loss of property**

238 Eq. 3 allows to calculate the annual risk of loss of property (R_p) caused by a potential natural hazard (in our
 239 case a tsunami event).

$$240 \quad R_p = P_{(H)} \times P_{(S:H)} \times P_{(T:S)} \times V \times E \quad (3)$$

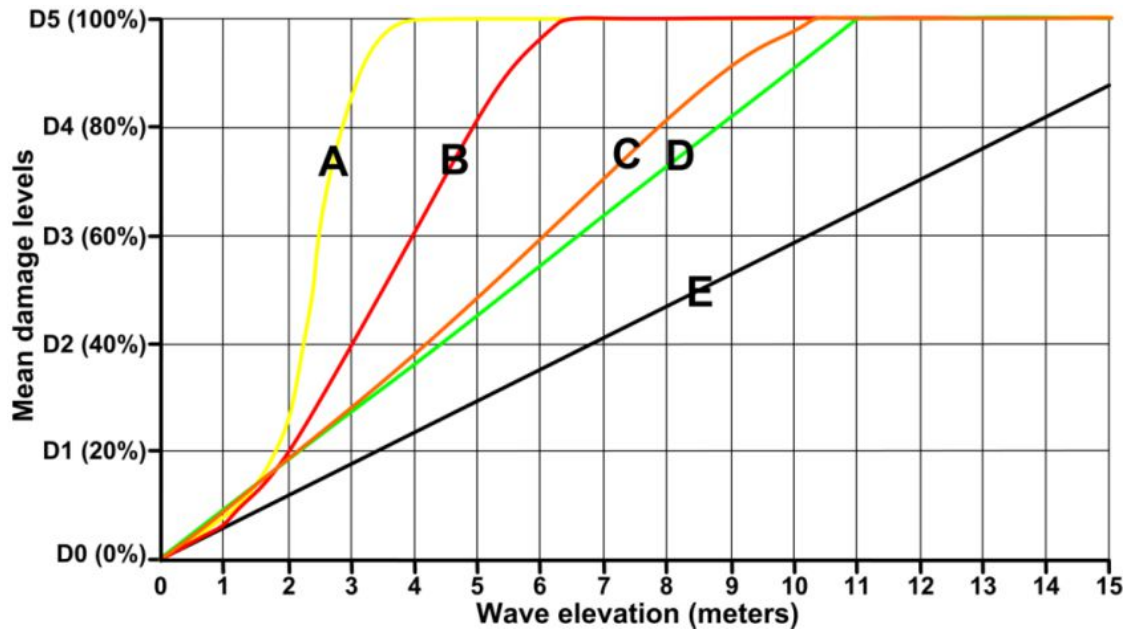
241 To calculate R_p using equation (3), the annual probability of the tsunami event $P_{(H)}$, the probability of its spatial
 242 impact given the hazardous event $P_{(S:H)}$, the probability of the element at risk being present along the path of the

243 flood $P_{(T,S)}$, the vulnerability of the exposed elements “V” and the estimated value of the property E must be
244 individually calculated.

245 In the Gulf of Cadiz, tsunamigenic earthquakes have mean recurrence period of 1000 years (Gutscher et al.
246 2006), yielding an annual probability ($P_{(H)}$) of 0.001. In the absence of an existing early warning center against
247 tsunamis (Birouk et al. 2020), we estimated that constructions, businesses and other assets couldn't be relocated
248 away from the risk area, which means that temporal probability of the consequence occurring is $P_{(T,S)}=1$. As for
249 $P_{(S,H)}$, the lack of a numerical estimation of the simulation results accuracy, means that its calculation could not
250 be objectively accomplished. However, we considered that the probability of spatial impact for all elements
251 reached by the flood is $P_{(S,H)}=1$, since reinforced-concrete buildings and all assets in the area cannot be displaced
252 in a short period of time.

253 To calculate the vulnerability of constructions to tsunamis, all buildings in the city were grouped into
254 homogenous residential blocks, which were then classified into five categories (A, B, C, D and E), following in
255 Atillah et al. (2011). This classification system was chosen because the building types and practices in El-Jadida
256 city and those of the areas investigated by these authors are similar. Therefore, the estimation of their
257 vulnerability can be achieved using the damage functions proposed by Gardi et al. (2009) (Fig. 6). To adapt this
258 model to the numerical input data format needed for equation (3), vulnerability classes presented in figure 6 were
259 converted to percentages (D0 = 0% damage, D1 = 20%; damage, D2 = 40%, D3 = 60%, D4 = 80%, and D5 =
260 100%) while the mean wave elevation for each block was derived from the simulation results. The obtained (V)
261 value was then attached to each individual block of buildings of the same type. The last input variable needed to
262 calculate $R(p)$ using equation (3) is the material value of the exposed buildings (E), which was obtained by
263 multiplying the reference unit-price for each square meter acquired from the real estate price assessment report
264 (D.G.I. 2015), by the total surface of each impacted residential block.

265 In addition to buildings, the road network is also a very important asset that must be included in R_p estimations.
266 In El-Jadida city, paved roads/streets are 243 km long. The unit price used in this study is 216\$ per km which is
267 a reasonable estimation of road cost in developing countries including Morocco (Collier et al. 2016). For
268 quantifying vulnerability of roads, a reference value of 60 % is used (Ginkel et al. 2021).



269

270 Figure 6: Damage functions for building classes A, B, C, D and E derived from experimental data from the area
 271 southwest of Banda Aceh (Sumatra, Indonesia) by GSC (modified after Gardi et al. 2009).

272 **3.2.2. Annual risk of loss of life**

273 Similarly to the annual risk of loss of property, the risk of loss of life $R_{(LoL)}$ can be estimated using the following
 274 equation:

275
$$R_{(LoL)} = P_H \times P_{(S:H)} \times P_{(T:S)} \times V \quad (4)$$

276 with the only difference being the mobility of the issues at stake and the equations system used for calculating
 277 their vulnerability. Hence, $P_{(T:S)}$ and V values are different from those used in equation (3). It is also important to
 278 note that the E value equals to 1 since the risk is calculated for each individual.

279 For calculating $P_{(T:S)}$, the concept of evacuation time t_e is adopted, which measures the time needed for a person
 280 to reach safe ground. This is important for estimating the number of people exposed to the tsunami wave. To
 281 quantify t_e , we used Eq.5, according to which evacuation time mainly depends on the distance from coast to safe
 282 ground (x_{max}), the distance from the coast to a person's location (x_0), the person's evacuation speed (c) and the
 283 time lapse between the tsunami occurrence and the beginning of evacuation (t_d) (Okumura et al.2017).

284
$$t_e = \frac{x_{max}-x_0}{c_e} + t_d \quad (5)$$

285 While x_{max} and x_0 can be automatically measured using a geographic information system (GIS) software, for
 286 inhabitants of each individual residential block, the evacuation c_e speed cannot be measured in the study area due
 287 to the absence of recent past events. For this reason, values estimated by Carey (2005) and adopted by Okumura
 288 et al. (2017) to perform QRA on the 2011 Okahura tsunami are also used in this study (Table.2). To adapt these
 289 reference values to the demography of El-Jadida, true population age percentage are used (HCP 2014) (Table.2).

290 In this respect, we propose the following Eq.6 to estimate $P_{(T:S)}$

$$291 \quad P_{(T:S)} = \frac{P_N + P_D}{2} \quad (6)$$

292 Where P_N is the probability of escaping the tsunami provided it occurred at night, and P_D is the same probability
 293 for a tsunami occurring during daytime. In the absence of an alarm system at the area (Birouk et al. 2020), we
 294 estimate that P_N is equal to 1 since most of the population will be inactive. For P_D values, a binary outcome is
 295 expected where persons able to escape the tsunami wave have a value of 0 and those unable to escape a value of
 296 1. To determine which zones are safe and which ones are not, we used the evacuation model proposed by
 297 Okumura et al. (2017).

298 However, not all persons exposed to the tsunami flood would be killed as demonstrated during the 2004 Asian
 299 tsunami, where a significant portion of the population survived the event. Accordingly, the V value depends on
 300 the probability of loss of life F_D , which could be estimated using equation 7 (CDMC 2003; Jonkman et al. 2008),
 301 with the only variable being the wave height (h) at the affected area:

$$302 \quad F_D = 0.0282e^{0.2328h} \quad F_D \leq 1 \quad (7)$$

303 Table 2: Evacuation speed and percentage of age categories in El-Jadida city

	Age distribution	Percentage of population	Evacuation speed (m/s)
Children	0-14	25,5	1.2
Average adult	15-64	69,8	1.38
Old/disabled	>65	4,7	1

304

305 4. Results

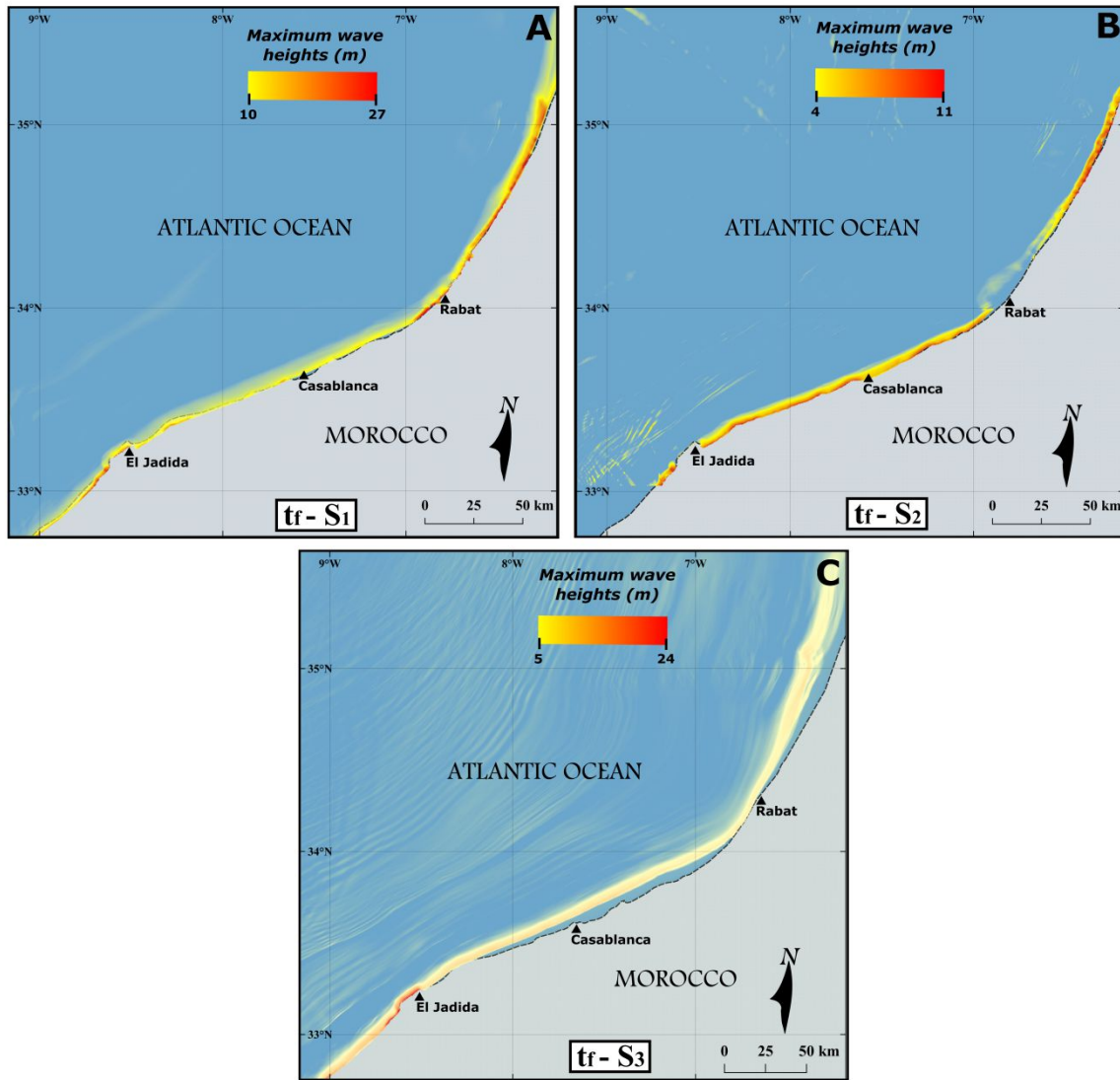
306 4.1. Tsunami waves propagation along the Moroccan Atlantic coast.

307 The tsunami simulations generated by MIRONÉ (Fig. 7) show that depending on the user provided fault
308 parameters used to define the source area, the maximum and minimum wave heights can vary significantly from
309 one model to the other (Fig. 7). Although studying the wave propagation along the whole length of the Moroccan
310 coast enables a better understanding of the near-field and far-field effects of the bathymetry on its mechanisms,
311 our description of the obtained results will essentially focus on the most important cities in this area.

312 In the first scenario, where the Horseshoe Fault is set as the tsunamigenic source, the maximum wave height
313 values range from 11 m to 27 m (Fig. 7). The highest waves would be recorded in Rabat, reaching up to 27 m in
314 the southern part of the city. To the north, the wave height would progressively decrease with values ranging
315 from 11 to 15 m. On the other hand, the lowest wave height would be recorded (11 to 12 m) in Casablanca and
316 its surrounding areas. To the south, waves arriving at the shoreline would reach heights of 20m or more.

317 In the second and least severe scenario (Marquês do Pombal Fault) (Fig.8-B), the maximum wave height values
318 range from 4 m to 11 m, with areas located in the north (Tangier and Larache) receiving the highest tsunami
319 waves (>8m). South of Casablanca, waves with heights reaching up to 9 m are also expected, while in Rabat
320 waves may reach roughly 4m.

321 The last scenario (Gorringe Bank Fault) (Fig.8-C) yields a wide range of wave height values with a maximum
322 and minimum of 24 m and 4 m respectively. However, the simulation stops before the leading propagating wave
323 reaches the center and northern segments of the shoreline. Reasons for this are discussed in section 5.1. In the
324 southern part of the study area, where the wave reaches the coast of El-Jadida city, the water elevation height
325 would attain 24 m. In other parts where the tsunami does not reach the coast, the wave heights are estimated to
326 be: (1) at least 6 m off the northern coasts, including Rabat; and (2) at least 9 m in Casablanca and the
327 neighboring coasts.



328

329

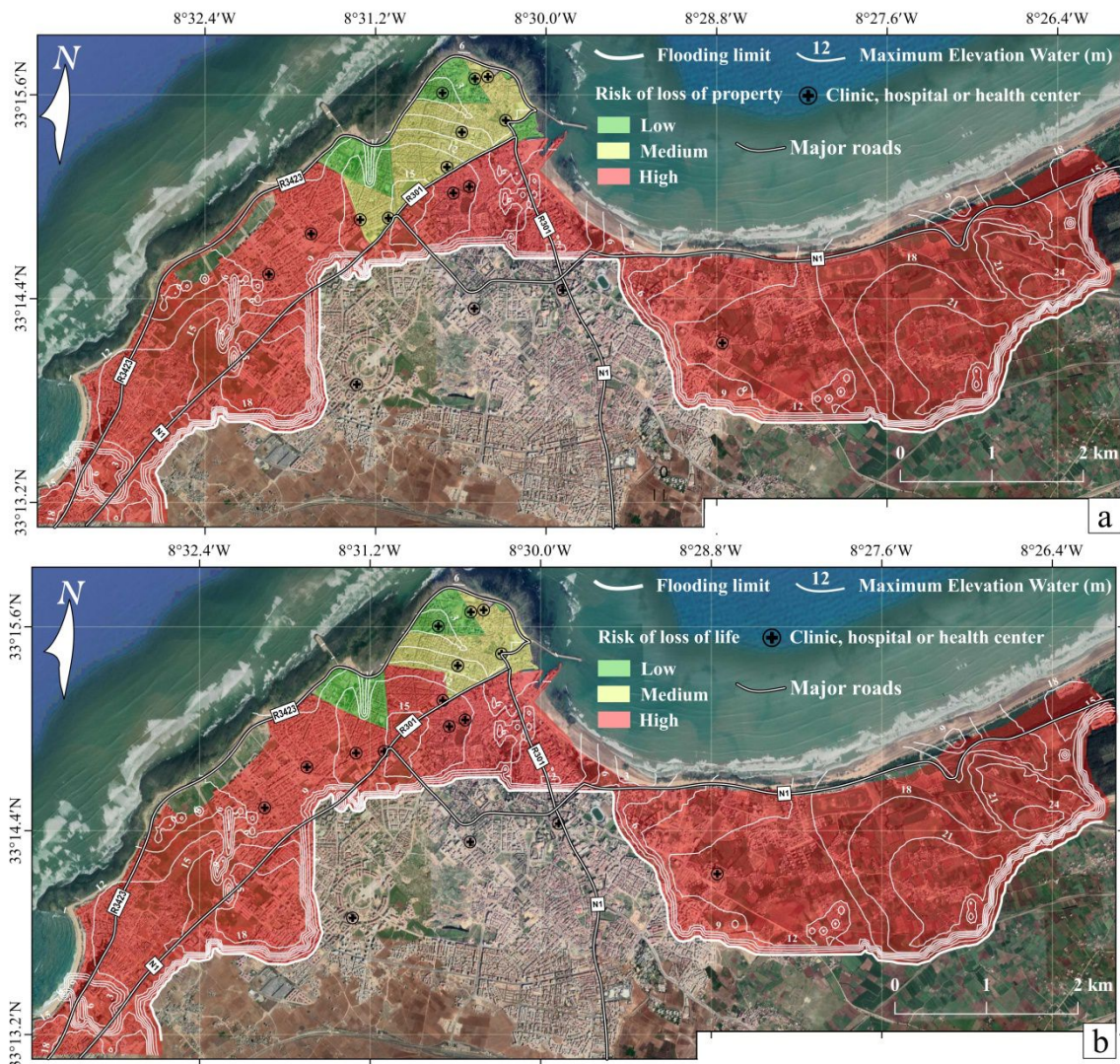
330 Figure 7: Maximum water elevation caused by the most credible earthquake scenarios in the Gulf of Cadiz
 331 region. A: Result of Horseshoe Fault scenario; B: Result of Marquês do Pombal Fault scenario; C: Result of
 332 Gorrige Bank Fault scenario. tf: final time for tsunami simulation; S: Scenario.

333 From the results obtained by this set of simulations, the Horseshoe Fault scenario produced the highest series of
 334 waves. For this reason, and because other authors (e.g. Pro et al. 2013; Buform et al. 2020) also consider it to be
 335 the most likely source for the 1755 event, it was used for QRA. A zoom on El Jadida city allows examining the
 336 tsunami run-up variation at the city-scale (Fig. 8).

337 **4.2. Building damage and human loss estimations for El-Jadida**

338 The QRA results show that most districts of El-Jadida city are highly exposed to tsunami risk (Fig. 8 and Table.
339 3). For the districts of Saada, Sidi Bouzid, Al Amal, Kaala and Al Jawhara/Sidi Moussa, the R_p is in excess of
340 one million dollars a year, which represents a very high economic cost to the population, especially when
341 considering the fragile socio-economic setting of El-Jadida city and that of Morocco in general (H.D.R. 2020).
342 At the city scale, the (R_p) amounts to more than 14M\$/yr, which constitutes a considerable risk to the economic
343 development of the city. Most of the elements at risk are buildings since the value of roads is found to be low in
344 comparison to other assets (31 k\$/yr). However these values of risk are only low because the return period of the
345 tsunami is very long, since one event could cost more than 14 B\$ only including direct damages.

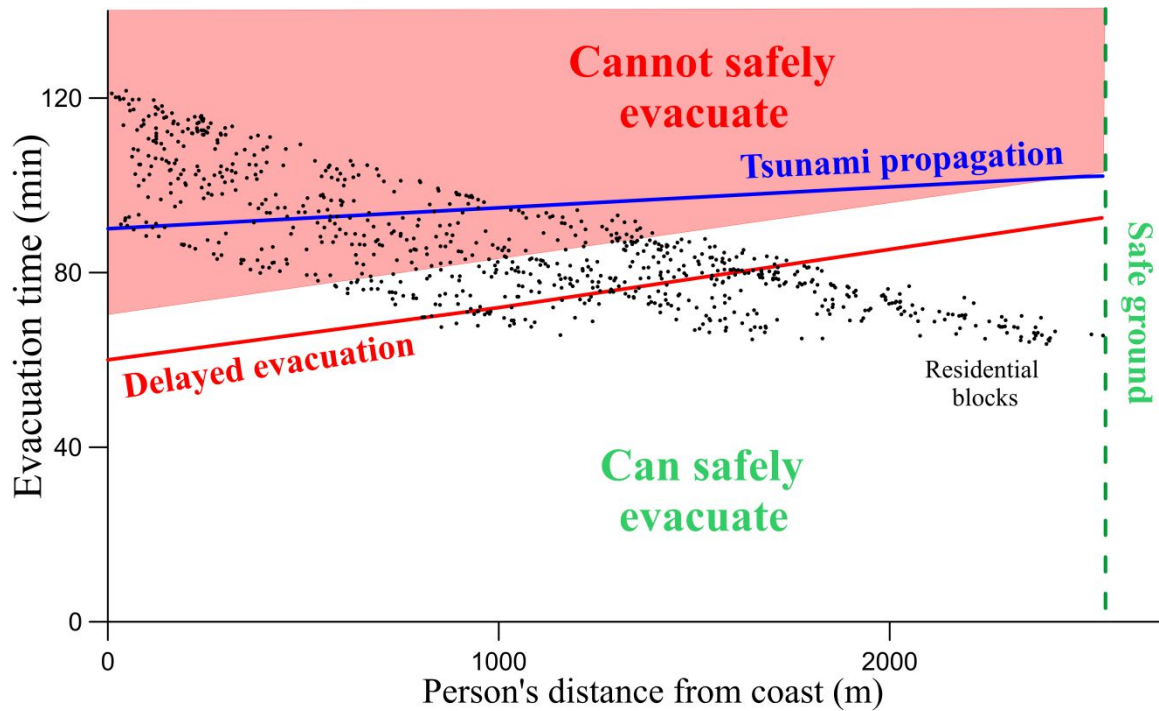
346 Although the assessment of economic risk is of importance, the R_{LOL} is the most crucial value to evaluate,
347 especially in the case of rapid onset, large-scale natural hazards such as tsunamis, which could claim hundreds of
348 thousands of lives in a matter of minutes. In the study area, the projection of residential bloc locations (where
349 most of the population is found) on the evacuation model (Fig.9) shows that 46% of the inundated zone can
350 safely evacuate if the tsunami were to occur in daytime and the evacuation were to start 60 min after the
351 triggering of tsunami waves or earlier. However, it is important to note that distances used for the projection of
352 residential blocs location relative to safe ground are calculated using the Manhattan approach. This accounts for
353 delays related to the geometry of buildings and the complexity of El-Jadida's road network. In the districts of Bir
354 Anzaran, Saada, Sidi Bouzid, Al Amal, Lala Zohra and El Jawhara/Sidi Moussa, R_{LOL} values exceed 10 lives/yr.
355 Although such values seem negligible when compared to the total number of residents in each district, it is
356 important to note that the temporal hazard of the simulated event is very low (0.1%). Thus, in the case of a
357 tsunami-generating earthquake like that of 1755, more than 34 000 (Table. 3) people could lose their lives.



358

359 Figure 8: Quantitative Risk estimation maps for El-Jadida city (source of background image: Google map

360 (<https://maps.google.com>) integrated in QGIS software as Basemap). **a.** R_p map. **b.** R_{LOL} map.



361

362 Figure 9: Projection of residential block locations and evacuation time on the Okumura et al. (2017) evacuation
 363 model. The black dots "represent vital infrastructure that is deemed essential to the rescue and evacuation
 364 operations".

365 Table 3: Quantitative risk estimation result for El-Jadida city. Red : high risk. Yellow: medium risk. Green: low
 366 risk.

District	Issues at stake (M\$)	Risk of loss of property (M\$/yr)	Issues at stake (Lives)	Risk of loss of life (Lives/yr)
<i>Sidi Daoui</i>	770.50	0.43	1536	0.15
<i>Mazagan</i>	2.29	0.00	687	0.09
<i>Mouilha</i>	-	-	-	-
<i>Biranzaran</i>	822.19	0.56	4392	2.08
<i>Saada</i>	2102.19	1.03	19670	3.85
<i>Sidi Bouzid</i>	1856.98	1.47	13155	7.08
<i>Amal</i>	2270.71	1.93	17938	4.21
<i>Salam</i>	-	-	-	-
<i>Derb Al Hajar</i>	4.53	0.09	2855	0.34
<i>Lala Zahra</i>	176.36	0.18	3844	2.31
<i>Derb Ghalef</i>	577.25	0.36	2118	0.29
<i>Kasr Lahmar</i>	3.94	0.00	-	-
<i>Kaala</i>	2381.14	1.86	16643	4.22
<i>El Kods</i>	-	-	-	-
<i>El Jawhara / Sidi Moussa (z)</i>	8546.49	6.54	26083	9.55

<i>Road network/Streets</i>	52.54	0.03	-	-
El Jadida	18744.07	14.48	108926	34.17

367

368 **5. Discussion**

369 **5.1. Limitations of the tsunami simulation**

370 Despite the data enhancement performed through several iterations in the MIRONE software, the relative low
371 resolution the GEBCO bathymetric/topographic data (300m) constitutes a limitation, especially when used for
372 city-scale hazard mapping. Therefore, the areas affected by the simulated tsunami could be off by dozens of
373 meters horizontally due to the simulation model dependence upon near source and regional bathymetry. Hence,
374 several artifacts related to over-shoots in the data, in areas of relatively steep topography (www.gebco.net) could
375 negatively impact the accuracy of the results. Also, small sub-marine canyons and manmade coastal structures
376 (port protection structures), which govern the form, amplitude, breaking wave points and the energy of the
377 tsunami, could be undetected because of the low-resolution of the input data. However, according to sub-marine
378 canyon maps of Morocco presented by Wynn et al. (2000), no small canyons, deep enough to be considered,
379 exist between the source area and El-Jadida city. Consequently, their effect on the results is deemed negligible at
380 best.

381 It is also important to note that parameters of active faults used to define the source areas for our simulations, are
382 based on investigations conducted on the 1755 event and recent earthquakes, in the Gulf of Cadiz (e.g., Johnston
383 1996; Hayward et al. 1999; Zitellini et al. 2001; Silva et al. 2017). The reason we only used the Horseshoe,
384 Goringe Bank and Marquês do Pombal faults for our simulations is their high spatio-temporal seismic hazard,
385 which has been demonstrated in many previous studies (Gutscher et al. 2006; Silva et al. 2017).

386 In addition, the inability of the simulation software to model wave propagation once tsunami travel time exceeds
387 6120s has proven to be a great challenge when the Goringe Bank Fault was defined as the source for the
388 tsunami generating earthquake (Fig.6-C). In our opinion, this is a significant limitation of this software
389 especially when tsunamigenic earthquakes occur far from the coast. Nevertheless, MIRONE could still be
390 considered a good tool for simulating near shore to medium range tsunami generating earthquake events, since
391 results of simulations 1 and 2 (Fig.6-A and B) have proven to be similar to those obtained using commercial
392 softwares (e.g. Omira et al., 2012).

393 Also, the magnitude calculated for the simulated event is in the order of 8.4, which is lower than values obtained
394 by Leet et al., (1950) (8.75 – 9) as well as those calculated by Levret (1991), Baptista et al. (1998) and Gutscher
395 et al. (2006) (8.5 – 9). However, recent efforts to estimate the magnitude of the 1755 event puts its value in a
396 range of (7.2 – 8.2), which is the closest to results obtained using equations 1 and 2 (see section 3).

397 Another limitation of the software used in this study is the necessity of making simplifying assumptions about
398 the source area's geometry and the number of fault segments responsible for the triggering event. Thus, we are
399 unable to simulate complex seismic scenarios such as the one proposed by Fonseca (2020), which invokes the
400 basal rupture of the Gulf of Cadiz accretionary prism as a cause for a seismic event in the Gulf of Cadiz. This
401 constraint might have an impact on the magnitude values calculated by the simulation software, and thus the
402 tsunami waves propagation and run-ups. However, we don't think that the difference will be significant enough
403 to radically change the QRA results. In addition, even commercial, state of the art softwares are unable to model
404 this type of scenario, which makes this not a software shortcoming, but rather a technical limitation needing to
405 be overcome.

406 According to our results, the wave heights in El-Jadida exceed 15 m and the tsunami wave inundation distance
407 reaches up to 1 km. These numbers are in agreement with historical testimonies (records) (Soyris 1755; El
408 Mrabet 2005), which were thought to be exaggerated, as well as recent computer simulation models (Mellas et
409 *al.* 2012). However, Omira et al. (2015) obtained different results. According to these authors and others (Omira
410 et al. 2012), wave heights values in excess of 10 meters should be regarded as over-estimated and unrealistic.
411 Despite this, we believe that an event of such proportions is possible since the old town of Mazagan, the
412 elevation of which exceeds 6 m, was impacted by the 1755 event.

413 **5.2. Reliability of the QRA method used in this study**

414 Although the QRA method proposed by Fell et al. (2005) takes into consideration all aspects of a given risk, it is
415 seldom used in tsunami studies (e.g. Li et al. 2021). Our results show that this system can yield interesting
416 results, allowing the assessment of economic and societal damages caused by tsunami events as well.
417 Nevertheless, one must note that because the exact location of the 1755 source area and its precise recurrence
418 interval remain uncertain, the calculated R_p and R_{LOL} values for El-Jadida city suffer from inaccuracies that
419 cannot be numerically quantified. Indeed, the recurrence period suggested by previous studies range from 300 to
420 2000 years (Ribeiro et al. 1996; Gutscher 2004; Ruiz et al. 2013), which means that the error if one extreme
421 value or the other were used could be important. For this reason, an intermediate value of 1000 years was
422 adopted in order to minimize the error and consequently avoid largely underestimating or overestimating the true

423 risk. In fact, this value is also at the low range of those generally agreed on regarding the current convergence
424 rates recorded in the Gulf of Cadiz (1cm/yr) (Gutscher *et al.* 2006).

425 In addition to inaccuracies in the spatio-temporal parameters of the natural hazard, errors related to the simulated
426 wave heights (discussed in section 5.1) influence the V value, which could, in some areas, lead to inaccurate
427 QRA of the true impact on buildings. Since the spatial errors of the topographic/bathymetric data are difficult to
428 quantify (www.gebco.net), their influence on the QRA results is consequently difficult to estimate. However, in
429 most areas of El-Jadida city, we consider that wave height values are large enough for us to deem vertical errors
430 in the input data irrelevant.

431 Moreover, one must stress the fact that this method only quantifies the value of property directly lost in
432 consequence to the catastrophic event. Nevertheless, rebuild efforts and debris clean-up operations cost, as well
433 as consequential damage to the regional economy of the area are not included in the QRA results. This is due to
434 a lack of recent tsunami occurrences alongside the Moroccan Atlantic shoreline which could serve as reference
435 points for the estimation. Despite the abundance of research elsewhere in the world, especially for the Japan
436 2011 tsunami (Ghaderi and Henderson 2013; Naito *et al.* 2014; Maximenko *et al.* 2018), the particularities of the
437 Moroccan economy makes it difficult to compare the results for both areas. In consequence, we consider that a
438 post-disaster rebuild and clean-up will cost as much as building a new city from scratch. To do so, the unit price
439 for urban infrastructure construction given in hectares is estimated to be around 1,3M\$ (MAUH 2012) which
440 accounts for a total of 16.9 M\$ for the affected area. For house reconstruction efforts, a unit price of 1000\$/m²
441 (Triantafyllou *et al.* 2018) is adopted to estimate the cost of rebuilding houses at the affected districts of El-
442 Jadida, which totals about 1.3 B\$.

443 Also, inaccuracies in R_{LOL} calculation using the Fell *et al.* (2005) method can result from the failure of this
444 system to incorporate the role of critical infrastructures and rescue and recovery efforts in reducing the tsunami
445 post-disaster impacts. For example it seems that most hospitals and care centers are located inside the flooded
446 area (Fig.8) which means that the injured must be transported hundreds of kilometers before receiving the care
447 they need. This constitutes a true logistical challenge for authorities, especially knowing that major road lines
448 connecting the city to other urban areas (N1 and R301) will also be partially inundated by the tsunami waves
449 (Fig.8). For this reason we propose constructing new healthcare centers in areas located away from high risk
450 zones in order to avoid casualties induced by logistical problems. Regarding the evacuation routes, the density of
451 urbanism and the non-regulated construction in many districts of the city constitute a true obstacle because of

452 socio-economic problems related to acquiring land property for the construction of such structures. In this
453 regard, we believe that the best solution is to install an operational early warning system and to educate the
454 population about the danger of tsunamis and the locations of safe zones if such events were to occur. Although
455 the most intuitive idea to protect the population against tsunamis is to build coastal defense structures, one
456 should consider the important height of tsunami waves at the area ($> 20\text{m}$) which is a true technical and
457 economic challenge for the state. A better alternative will be the design of vertical evacuation structures in high
458 risk areas in a way that allows the rapid evacuation of most people living in these districts. Ideas for the planning
459 and design of such structures are proposed by Heintz and Robertson (2008); Park et al.(2012) and Wood et al.
460 (2014).

461 Regarding the geographic distribution of high and low risk areas (Table. 3) (Fig.8), it seems that despite their
462 closeness to the shoreline, many districts such as Mazagan, Mouilha, Salam, Kasr Lahmar and El Kods are low-
463 risk. This is because these districts were built on the rocky Cape Mazagan, which acts as a natural barrier that
464 dissipates the tsunami waves energy and thus decreases tsunami impact on the shore.

465 **6. Conclusion**

466 In the Gulf of Cadiz, Marquês do Pombal, Gorringe Bank and Horseshoe faults could trigger tsunamis in the
467 future. According to our simulation results, out of the three the Horseshoe Fault could produce the largest
468 tsunami. For this reason, and because of its relation to recent and old events of significance, this fault was picked
469 as the most likely source of a potential tsunami. However, despite the differences between previous simulations
470 and those performed in this study, the results obtained agree on the fact that the northern Atlantic coast of
471 Morocco is highly exposed to the tsunami hazard, which could impact areas with high population densities and
472 economic interests.

473 For El-Jadida city, QRA results show that such events could be disastrous especially in the districts of Saada,
474 Sidi Bouzid, Amal, Kaala and El Jawhara / Sidi Moussa, which are thus very high-risk areas. On the other hand,
475 and despite its closeness to the shoreline, the Mazagan district, built on a low-elevation rocky cape might be less
476 affected. Based on these results, we recommend establishing a tsunami response and mitigation strategy that,
477 should allow for a quicker and more accurate intervention in the case of a future extreme event. The basis of
478 such a strategy must include but not be limited to the installation of an effective early response system, the

479 education of the coastal population about the dangers of tsunamis and the most exposed areas and the
480 construction (if possible) of vertical tsunami evacuation structures.

481 **Highlights**

- 482 - Multi-assessment of the impacts of tsunami along the northern Atlantic coast of Morocco.
- 483 - Quantitative Risk Assessment to calculate the loss of property and life in El-Jadida city.

484 **Acknowledgment**

485 This work is part of the RiskMED project, Labex OT-Med (ANR-11-LABE-0061), supported by the
486 Investissements d'Avenir, French Government project of the French National Research Agency (ANR) through
487 the A*Midex project (ANR-1-IE-0001-02). The authors acknowledge the Editors for their help during the
488 manuscript review and submission process. The authors also thank all the reviewers for their constructive and
489 valuable comments. In like manner, the authors thank Edward Anthony for his help in improving the overall
490 quality of the English writing of this paper.

491 **Declaration of competing Interest**

492 The authors declare that they do not have any personal relationships or financial interests that influence the work
493 reported in this paper.

494 **References**

- 495 Aki K (1966) Generation and Propagation of G Waves from the Niigata Earthquake of June 16, 1964. Bull.
496 Earthq. Res. Inst. 44
- 497 Atillah A, Hadani D El, Moudni H, Lesne O, Renou C, Mangin A, Rouffi F (2011) Tsunami vulnerability
498 and damage assessment in the coastal area of Rabat and Salé, Morocco. Nat Hazards Earth Syst Sci
499 11:. <https://doi.org/10.5194/nhess-11-3397-2011>
- 500 Baptista MA, Miranda P, Victor LM (1992) Maximum entropy analysis of Portuguese tsunami data. The
501 tsunamis of 28.02.1969 and 26.05.1975. Sci Tsunami Hazards 10:9–20
- 502 Baptista MA, Miranda PMA, Miranda JM, Victor LM (1998) Constrains on the source of the 1755 Lisbon
503 tsunami inferred from numerical modelling of historical data on the source of the 1755 Lisbon
504 tsunami. J Geodyn 25:. [https://doi.org/10.1016/s0264-3707\(97\)00020-3](https://doi.org/10.1016/s0264-3707(97)00020-3)
- 505 Barkan R, ten Brink US, Lin J (2009) Far field tsunami simulations of the 1755 Lisbon earthquake:
506 Implications for tsunami hazard to the U.S. East Coast and the Caribbean. Mar Geol 264:.
507 <https://doi.org/10.1016/j.margeo.2008.10.010>
- 508 Bartolome R, Gràcia E, Stich D, Martínez-Loriente S, Klaeschen D, de Lis Mancilla F, Iacono C Lo,
509 Dañobeitia JJ, Zitellini N (2012) Evidence for active strike-slip faulting along the Eurasia-Africa
510 convergence zone: Implications for seismic hazard in the southwest Iberian margin. Geology 40:.
511 <https://doi.org/10.1130/G33107.1>
- 512 Bernard EN, Behn RR, Hebenstreit GT, Gonzalez FI, Krumpe P, Lander JF, Lorca E, McManamon PM,
513 Milburn HB (1988) On mitigating rapid onset natural disasters: Project THRUST (Tsunami Hazards
514 Reduction Utilizing Systems Technology). Eos, Trans Am Geophys Union 69:.
515 <https://doi.org/10.1029/88EO00208>
- 516 Birouk A, Ibenbrahim A, Mouraouah A El, Kasmi M (2020) New integrated networks for monitoring
517 seismic and tsunami activity in Morocco. Ann Geophys 63:. <https://doi.org/10.4401/AG-7954>
- 518 Blanc PL (2009) Earthquakes and Tsunami in November 1755 in Morocco: A different reading of

519 contemporaneous documentary sources. *Nat Hazards Earth Syst Sci* 9:. <https://doi.org/10.5194/nhess->
520 9-725-2009

521 Buform E, López-Sánchez C, Lozano L, Martínez-Solares JM, Cesca S, Oliveira CS, Udías A (2020) Re-
522 evaluation of Seismic Intensities and Relocation of 1969 Saint Vincent Cape Seismic Sequence: A
523 Comparison with the 1755 Lisbon Earthquake. *Pure Appl Geophys* 177:.
524 <https://doi.org/10.1007/s00024-019-02336-8>

525 Carey N (2005) Establishing pedestrian walking speeds. Portland State University, ITE Student Chapter.

526 Cavallo E, Galiani S, Noy I, Pantano J (2013) Catastrophic natural disasters and economic growth. *Rev*
527 *Econ Stat* 95:. https://doi.org/10.1162/REST_a_00413

528 Cavallo E, Noy I (2011) Natural disasters and the economy - A survey. *Int Rev Environ Resour Econ* 5:.
529 <https://doi.org/10.1561/101.00000039>

530 CDMC (Central Disaster Management Council) (2003) Damage estimation method for the Tonankai and
531 Nankai Earthquakes. Cabinet Office, Government of Japan, Tokyo.

532 Collier P, Kirchberger M, Söderbom M (2016) The Cost of Road Infrastructure in Low- and Middle-
533 Income Countries. *World Bank Econ Rev* 30:522–548. <https://doi.org/10.1093/WBER/LHV037>

534 Cunha PP, Buylaert JP, Murray AS, Andrade C, Freitas MC, Fatela F, Munhá JM, Martins AA, Sugisaki S
535 (2010) Optical dating of clastic deposits generated by an extreme marine coastal flood: The 1755
536 tsunami deposits in the Algarve (Portugal). *Quat Geochronol* 5:.
537 <https://doi.org/10.1016/j.quageo.2009.09.004>

538 DAT (Direction de l'Aménagement du Territoire) (2017) Élaboration de la stratégie nationale de gestion
539 intégrée du littoral - Phase 2: Diagnostic stratégique du littoral.
540 <https://www.muat.gov.ma/sites/default/files/Documentation/17.pdf>. Accessed 6 Oct 2021

541 DGI (Direction Générale des Impôts) (2015) Rapport d'activité.
542 https://www.finances.gov.ma/Publication/dgi/2017/rapport_dgi_2015.pdf. Accessed January 2020.
543 Accessed 20 Apr 2021

- 544 Doocy S, Gorokhovich Y, Burnham G, Balk D, Robinson C (2007) Tsunami mortality estimates and
545 vulnerability mapping in Aceh, Indonesia. *Am J Public Health* 97 Suppl 1:
546 <https://doi.org/10.2105/AJPH.2006.095240>
- 547 Ekström G, Nettles M, Dziewoński AM (2012) The global CMT project 2004-2010: Centroid-moment
548 tensors for 13,017 earthquakes. *Phys Earth Planet Inter* 200–201:
549 <https://doi.org/10.1016/j.pepi.2012.04.002>
- 550 El Mrabet T (2005) The great earthquakes in the Maghreb region and their consequences on man and
551 environment. Rabat. ISBN- 9954-0-3777-2
- 552 Fell R, Ho KKS, Lacasse S, Leroi E (2005) State of the Art Paper 1 A framework for landslide risk
553 assessment and management. *Int Conf Landslide Risk Manag Vancouver, Canada*
- 554 Fonseca JFBD (2020) A reassessment of the magnitude of the 1755 Lisbon earthquake. *Bull Seismol Soc*
555 *Am* 110:. <https://doi.org/10.1785/0120190198>
- 556 Font E, Nascimento C, Omira R, Baptista MA, Silva PF (2010) Identification of tsunami-induced deposits
557 using numerical modeling and rock magnetism techniques: A study case of the 1755 Lisbon tsunami
558 in Algarve, Portugal. *Phys Earth Planet Inter* 182:. <https://doi.org/10.1016/j.pepi.2010.08.007>
- 559 Fukao Y (1973) Thrust faulting at a lithospheric plate boundary the Portugal earthquake of 1969. *Earth*
560 *Planet Sci Lett* 18:. [https://doi.org/10.1016/0012-821X\(73\)90058-7](https://doi.org/10.1016/0012-821X(73)90058-7)
- 561 Gardi A, Valencia N, Sheer S (2009) WP3.3 – GIS conceptual model and processing for production of
562 elements required for test sites scenarios, Deliverable 3.1 part II, SCHEMA project.
- 563 Ghaderi Z, Henderson JC (2013) Japanese tsunami debris and the threat to sustainable tourism in the
564 Hawaiian Islands. *Tour Manag Perspect* 8:98–105. <https://doi.org/10.1016/J.TMP.2013.09.001>
- 565 Ginkel KCH Van, Dottori F, Alfieri L, Feyen L, Koks EE (2021) Flood risk assessment of the European
566 road network. *Nat Hazards Earth Syst Sci* 21:1011–1027. [https://doi.org/10.5194/NHESS-21-1011-](https://doi.org/10.5194/NHESS-21-1011-2021)
567 2021
- 568 Gràcia E, Danobeitia J, Vergés J, Bartolomé R, Córdoba D (2003) Crustal architecture and tectonic

569 evolution of the Gulf of Cadiz (SW Iberian margin) at the convergence of the Eurasian and African
570 plates. *Tectonics* 22:. <https://doi.org/10.1029/2001tc901045>

571 Granger K, Jones T, Leiba M, Scott G (1998) Community risk in Cairns: A multi-hazard risk assessment.
572 *Aust J Emerg Manag* 13:

573 Gutscher MA (2004) What caused the Great Lisbon earthquake? *Science* (80-) 305:1247–1248.
574 <https://doi.org/10.1126/science.1101351>

575 Gutscher MA, Baptista MA, Miranda JM (2006) The Gibraltar Arc seismogenic zone (part 2): Constraints
576 on a shallow east dipping fault plane source for the 1755 Lisbon earthquake provided by tsunami
577 modeling and seismic intensity. *Tectonophysics* 426:. <https://doi.org/10.1016/j.tecto.2006.02.025>

578 Hanks TC, Kanamori H (1979) A moment magnitude scale. *J Geophys Res B Solid Earth* 84:2348–2350.
579 <https://doi.org/10.1029/JB084iB05p02348>

580 Hayward N, Watts AB, Westbrook GK, Collier JS (1999) A seismic reflection and GLORIA study of
581 compressional deformation in the Gorringe Bank region, eastern North Atlantic. *Geophys J Int* 138:.
582 <https://doi.org/10.1046/j.1365-246X.1999.00912.x>

583 HCP (Haut Commicariat au Plan) (2014) Recensement général de la population humaine.
584 <http://rgphentableaux.hcp.ma/Default1/>. Accessed 6 Apr 2021

585 HDR (2020) Human Development Report 2020. <http://www.hdr.undp.org/sites/default/files/hdr2020.pdf>.
586 Accessed 15 Oct 2021

587 Heger MP, Neumayer E (2019) The impact of the Indian Ocean tsunami on Aceh’s long-term economic
588 growth. *J Dev Econ* 141:. <https://doi.org/10.1016/j.jdeveco.2019.06.008>

589 Heintz JA, Robertson IN (2008) Design of Structures for Vertical Evacuation from Tsunamis. *Solut to*
590 *Coast Disasters Congr 2008 Tsunamis - Proc Solut to Coast Disasters Congr 2008 Tsunamis* 313:72–
591 81. [https://doi.org/10.1061/40978\(313\)7](https://doi.org/10.1061/40978(313)7)

592 ISC (International Seismological Centre (2020) On-line Bulletin.
593 <https://earthquake.usgs.gov/earthquakes/search/>. Accessed 11 Dec 2020

594 Jelínek R, Krausmann E (2008) Approaches to tsunami risk assessment. JRC Scientific and Technical
595 Reports, 48713.

596 Jelínek R, Krausmann E, González M, Álvarez-Gómez JA, Birkmann J, Welle T (2012) Approaches for
597 tsunami risk assessment and application to the city of Cádiz, Spain. *Nat. Hazards* 60

598 Johnston AC (1996) Seismic moment assessment of earthquakes in stable continental regions - I.
599 Instrumental seismicity. *Geophys J Int* 124:. <https://doi.org/10.1111/j.1365-246X.1996.tb07028.x>

600 Jonkman SN, Vrijling JK, Vrouwenvelder ACWM (2008) Methods for the estimation of loss of life due to
601 floods: A literature review and a proposal for a new method. *Nat. Hazards* 46

602 Khalfaoui O, Dezileau L, Degeai JP, Snoussi M (2020) A late Holocene record of marine high-energy
603 events along the Atlantic coast of Morocco: new evidences from the Tahaddart estuary.
604 *Geoenvironmental Disasters* 7:. <https://doi.org/10.1186/s40677-020-00169-5>

605 Laouina A (2019) Note de recherche – Le littoral dans le développement du Maroc et de sa politique
606 atlantique. *Norois*. <https://doi.org/10.4000/norois.9351>

607 Leet LD, Gutenberg B, Richter CF (1950) Seismicity of the Earth and Associated Phenomena. *Geogr Rev*
608 40:. <https://doi.org/10.2307/211302>

609 Levret A (1991) The effects of the November 1, 1755 “Lisbon” earthquake in Morocco. *Tectonophysics*
610 193:. [https://doi.org/10.1016/0040-1951\(91\)90190-4](https://doi.org/10.1016/0040-1951(91)90190-4)

611 Li XH, Zheng JC (2014) Efficient post-disaster patient transportation and transfer: experiences and lessons
612 learned in emergency medical rescue in Aceh after the 2004 Asian tsunami. *Mil Med* 179:.
613 <https://doi.org/10.7205/MILMED-D-13-00525>

614 Li Y, Chen L, Yin K, Zhang Y, Gui L (2021) Quantitative risk analysis of the hazard chain triggered by a
615 landslide and the generated tsunami in the Three Gorges Reservoir area. *Landslides* 18:.
616 <https://doi.org/10.1007/s10346-020-01516-1>

617 Loayza N V, Olaberria E, Rigolini J, Christiaensen L (2012) Natural Disasters and Growth: Going Beyond
618 the Averages. *World Dev* 40:. <https://doi.org/10.1016/j.worlddev.2012.03.002>

619 Luis JF (2007) Mirone: A multi-purpose tool for exploring grid data. *Comput Geosci* 33:.
620 <https://doi.org/10.1016/j.cageo.2006.05.005>

621 Mansinha L, Smylie DE (1971) The displacement fields on inclined faults. *Bull Seism Soc Am* 61:

622 Martínez-Loriente S, Gràcia E, Bartolome R, Perea H, Klaeschen D, Dañobeitia JJ, Zitellini N, Wynn RB,
623 Masson DG (2018) Morphostructure, tectono-sedimentary evolution and seismic potential of the
624 Horseshoe Fault, SW Iberian Margin. *Basin Res* 30:.. <https://doi.org/10.1111/bre.12225>

625 Matias LM, Cunha T, Annunziato A, Baptista MA, Carrilho F (2013) Tsunamigenic earthquakes in the
626 Gulf of Cadiz: Fault model and recurrence. *Nat Hazards Earth Syst Sci* 13:.
627 <https://doi.org/10.5194/nhess-13-1-2013>

628 MAUH (2012) (Ministère de l'Aménagement de l'Urbanisme et de l'Habitat): Etude relative au
629 financement et à la maîtrise du coût de l'urbanisation.
630 <https://www.muat.gov.ma/sites/default/files/Documentation/17.pdf>. Accessed 15 Oct 2021

631 Maximenko N, Hafner J, Kamachi M, MacFadyen A (2018) Numerical simulations of debris drift from the
632 Great Japan Tsunami of 2011 and their verification with observational reports. *Mar Pollut Bull*
633 132:5–25. <https://doi.org/10.1016/J.MARPOLBUL.2018.03.056>

634 Medina F, Mhammdi N, Chiguer A, Akil M, Jaaidi EB (2011) The Rabat and Larache boulder fields; new
635 examples of high-energy deposits related to storms and tsunami waves in north-western Morocco.
636 *Nat Hazards* 59:.. <https://doi.org/10.1007/s11069-011-9792-x>

637 Mellas S, Leone F, Omira R, Gherardi M, Baptista M-A, Zourarah B, Péroche M, Lagahé É (2012) Le
638 risque tsunamique au Maroc : modélisation et évaluation au moyen d'un premier jeu d'indicateurs
639 d'exposition du littoral atlantique. *Physio-Géo*. <https://doi.org/10.4000/physio-geo.2589>

640 Mhammdi N, Medina F (2015) Recent Tsunami Deposits Along the Moroccan Atlantic Coast. In: XIV
641 Reunión Nacional de Cuaternario. Granada

642 Moussaoui S El, Omira R, Zaghoul MN, Talibi H El, Aboumaria K (2017) Tsunami hazard and buildings
643 vulnerability along the Northern Atlantic coast of Morocco –the 1755-like tsunami in Asilah test-site.
644 *Geoenvironmental Disasters* 4:.. <https://doi.org/10.1186/s40677-017-0089-6>

645 Nadim F (2006) On Tsunami Risk Assessment for the West Coast of Thailand. *Geohazards Eng Conf Int*

646 Naito C, Cercone C, Riggs HR, Cox D (2014) Procedure for Site Assessment of the Potential for Tsunami
647 Debris Impact. *J Waterw Port, Coastal, Ocean Eng* 140:223–232.
648 [https://doi.org/10.1061/\(ASCE\)WW.1943-5460.0000222](https://doi.org/10.1061/(ASCE)WW.1943-5460.0000222)

649 Okumura N, Jonkman SN, Esteban M, Hofland B, Shibayama T (2017) A method for tsunami risk
650 assessment: a case study for Kamakura, Japan. *Nat Hazards* 2017 883 88:1451–1472.
651 <https://doi.org/10.1007/S11069-017-2928-X>

652 Omira R, Baptista MA, Matias L, Miranda JM, Catita C, Carrilho F, Toto E (2009) Design of a sea-level
653 tsunami detection network for the Gulf of Cadiz. *Nat Hazards Earth Syst Sci* 9:.
654 <https://doi.org/10.5194/nhess-9-1327-2009>

655 Omira R, Baptista MA, Miranda JM, Toto E, Catita C, Catalão J (2010) Tsunami vulnerability assessment
656 of Casablanca-Morocco using numerical modelling and GIS tools. *Nat Hazards* 54:.
657 <https://doi.org/10.1007/s11069-009-9454-4>

658 Omira R, Baptista MA, Mellas S, Leone F, de Richemond NM, Zourarah B, Cherel J-P (2012) The
659 November, 1st, 1755 Tsunami in Morocco: Can Numerical Modeling Clarify the Uncertainties of
660 Historical Reports? In: *Tsunami - Analysis of a Hazard - From Physical Interpretation to Human*
661 *Impact*. IntechOpen, pp 61–76

662 Omira R, Baptista MA, Leone F, Matias L, Mellas S, Zourarah B, Miranda JM, Carrilho F, Cherel JP
663 (2013) Performance of coastal sea-defense infrastructure at El Jadida (Morocco) against tsunami
664 threat: Lessons learned from the Japanese 11 March 2011 tsunami. *Nat Hazards Earth Syst Sci* 13:.
665 <https://doi.org/10.5194/nhess-13-1779-2013>

666 Omira R, Baptista MA, Matias L (2015) Probabilistic Tsunami Hazard in the Northeast Atlantic from Near-
667 and Far-Field Tectonic Sources. *Pure Appl Geophys* 172:.. <https://doi.org/10.1007/s00024-014-0949-x>

668 Papatoma M, Dominey-Howes D, Zong Y, Smith D (2003) Assessing tsunami vulnerability, an example
669 from Herakleio, Crete. *Nat Hazards Earth Syst Sci* 3:.. <https://doi.org/10.5194/nhess-3-377-2003>

670 Park S, van de Lindt JW, Gupta R, Cox D (2012) Method to determine the locations of tsunami vertical

671 evacuation shelters. *Nat Hazards* 2012 63:891–908. <https://doi.org/10.1007/S11069-012-0196-3>

672 Post J, Wegscheider S, Mück M, Zosseder K, Kiefl R, Steinmetz T, Strunz G (2009) Assessment of human
673 immediate response capability related to tsunami threats in Indonesia at a sub-national scale. *Nat*
674 *Hazards Earth Syst Sci* 9:1075–1086. <https://doi.org/10.5194/NHESS-9-1075-2009>

675 Pro C, Buforn E, Bezzeghoud M, Udías A (2013) The earthquakes of 29 July 2003, 12 February 2007, and
676 17 December 2009 in the region of Cape Saint Vincent (SW Iberia) and their relation with the 1755
677 Lisbon earthquake. *Tectonophysics* 583:.. <https://doi.org/10.1016/j.tecto.2012.10.010>

678 Ramalho I, Omira R, Moussaoui S El, Baptista MA, Zaghoul MN (2018) Tsunami-induced morphological
679 change – A model-based impact assessment of the 1755 tsunami in NE Atlantic from the Morocco
680 coast. *Geomorphology* 319:.. <https://doi.org/10.1016/j.geomorph.2018.07.013>

681 Renou C, Lesne O, Mangin A, Rouffi F, Atillah A, Hadani D El, Moudni H (2011) Tsunami hazard
682 assessment in the coastal area of Rabat and Salé, Morocco. *Nat Hazards Earth Syst Sci* 11:..
683 <https://doi.org/10.5194/nhess-11-2181-2011>

684 Ribeiro A, Cabral J, Baptista R, Matias L (1996) Stress pattern in Portugal mainland and the adjacent
685 Atlantic region, West Iberia. *Tectonics* 15:.. <https://doi.org/10.1029/95TC03683>

686 Ruiz F, Rodríguez-Vidal J, Abad M, Cáceres LM, Carretero MI, Pozo M, Rodríguez-Llanes JM, Gómez-
687 Toscano F, Izquierdo T, Font E, Toscano A (2013) Sedimentological and geomorphological imprints
688 of Holocene tsunamis in southwestern Spain: An approach to establish the recurrence period.
689 *Geomorphology* 203:.. <https://doi.org/10.1016/j.geomorph.2013.09.008>

690 Saunders W, Glassey P (2007) Guidelines for assessing planning policy and consent requirements for
691 landslide prone land. *GNS Sci. Misc. Ser.* 7

692 Scholz CH (1981) Scaling laws for large earthquakes; consequences for physical models. *Bull Seismol Soc*
693 *Am* 72:1–14

694 Sharpley R (2005) The tsunami and tourism: A comment. *Curr. Issues Tour.* 8

695 Silva S, Terrinha P, Matias L, Duarte JC, Roque C, Ranero CR, Geissler WH, Zitellini N (2017) Micro-

696 seismicity in the Gulf of Cadiz: Is there a link between micro-seismicity, high magnitude earthquakes
697 and active faults? *Tectonophysics* 717:226–241. <https://doi.org/10.1016/J.TECTO.2017.07.026>

698 Solares JMM, Arroyo AL (2004) The great historical 1755 earthquake. Effects and damage in Spain. *J*
699 *Seismol* 8:. <https://doi.org/10.1023/B:JOSE.0000021365.94606.03>

700 Soyris M (1755) Extrait d'une lettre de Maroc en date du 5 novembre 1755 : de Soyris à Guys. *Archives N*:

701 Talibi H El, Moussaoui S El, Zaghoul MN, Aboumaria K, Wassmer P, Mercier JL (2016) New
702 sedimentary and geomorphic evidence of tsunami flooding related to an older events along the
703 Tangier-Asilah coastal plain, Morocco. *Geoenvironmental Disasters* 3:.
704 <https://doi.org/10.1186/s40677-016-0049-6>

705 Triantafyllou I, Novikova T, Charalampakis M, Fokaefs A, Papadopoulos GA (2018) Quantitative Tsunami
706 Risk Assessment in Terms of Building Replacement Cost Based on Tsunami Modelling and GIS
707 Methods: The Case of Crete Isl., Hellenic Arc. *Pure Appl Geophys* 2018 1767 176:3207–3225.
708 <https://doi.org/10.1007/S00024-018-1984-9>

709 UNESCO (2004) World Heritage List. <https://whc.unesco.org/fr/list/1058/>. Accessed 10 Feb 2021

710 Wood N, Jones J, Schelling J, Schmidlein M (2014) Tsunami vertical-evacuation planning in the U.S.
711 Pacific Northwest as a geospatial, multi-criteria decision problem. *Int J Disaster Risk Reduct* 9:68–
712 83. <https://doi.org/10.1016/J.IJDRR.2014.04.009>

713 Wynn RB, Masson DG, Stow DA V, Weaver PPE (2000) The Northwest African slope apron: A modern
714 analogue for deep-water systems with complex seafloor topography. *Mar Pet Geol* 17:.
715 [https://doi.org/10.1016/S0264-8172\(99\)00014-8](https://doi.org/10.1016/S0264-8172(99)00014-8)

716 Zitellini N, Chierici F, Sartori R, Torelli L (1999) The tectonic source of the 1755 Lisbon earthquake and
717 tsunamis. *Ann di Geofis* 42:

718 Zitellini N, Mendes LA, Cordoba D, Danobeitia J, Nicolich R, Pellis G, Ribeiro A, Sartori R, Torelli L,
719 Bartolome R, Bortoluzzi G, Calafato A, Carrilho F, Casoni L, Chierici E, Corela C, Correggiari A,
720 Vedova BD, Gracia E, Jornet P, Landuzzi M, Ligi M, Magagnoli A, Marozzi G, Matias L, Penitenti
721 D, Rodriguez P, Rovere M, Terrinha P, Vigliotti L, Ruiz, A Zahinos (2001) Source of 1755 lisbon

722 earthquake and tsunami investigated. Eos (Washington DC) 82:.

723 <https://doi.org/10.1029/EO082i026p00285-01>

724